

KNOWLEDGE-BASED DESIGN FOR FUTURE COMBAT AIRCRAFT CONCEPTS

Raghu Chaitanya Munjulury*, Ingo Staack*, Alvaro Abdalla**, Tomas Melin*, Christopher Jouannet*, Petter Krus*

*Linköping University, Linköping, Sweden

**USP, Sao Carlos, Brazil

Keywords: *Conceptual design, Aircraft design, Engine design, Knowledge-based*

Abstract

A new fighter aircraft will most likely be a collaborative project. In this study conceptual knowledge-based design is demonstrated, using models of comparable fidelity for sizing, geometry design, aerodynamic analysis and system simulation for aircraft conceptual design. A new generation fighter is likely to involve advanced control concept where an assessment of feasibility through simulation is needed already at the conceptual stage. This co-design leads to a deeper understanding of the trade-offs involved. In this paper a study for a future combat aircraft is made. Conceptual knowledge-based design is demonstrated by optimizing for a design mission, including a super-cruise segment.

1 Introduction

In object for this design study a future combat aircraft with a hypothetical time of deployment in 2030. Within this time frame an enormous amount of development will take place. Nevertheless, considering the time frames involved in aircraft design means that the initiation of such a project would not be far off. The aircraft under study is a stealth design with super-cruise capability. The aircraft have provision to carry a pilot, although an unmanned version is also possible. The concept is relatively small for two reasons. First, size drives cost and therefore the market for small aircraft should be bigger, second, payload tend to become more efficient over time mean-

ing that a high capability can be obtained also in a small platform. Furthermore, a small aircraft has inherently smaller signature and more agility than a large one. In this case the empty weight is set to 7000 kg and the maximum takeoff weight is 9000 kg. The reference area of the wing is 32 m². In order to minimize drag and signature, there is no vertical tail. To achieve high maneuverability there is thrust vectoring. This also adds the capability of high AOA landings [1], as well as quicker rotation on take-off producing STOL capability. Since thrust vectoring is inefficient in the absent of thrust, additional yaw control is achieved with differential canard, and with differential/split elevons as shown in Fig. 1.

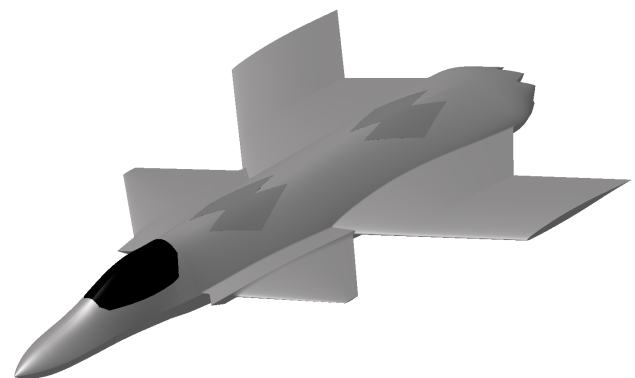


Fig. 1 : Baseline design for Combat aircraft with no-vertical tail design.

For the aircraft design the software suite of Tango, RAPID, Tornado, and Hopsan are used. For the engine design a generic engine model is used, this engine is adapted to suit the aircraft capability. Tango is used for the initial sizing and

RAPID, which is a CATIA based tool, for the more detailed geometric design, and in particular for estimation of area distribution and wave drag estimation. Tornado is used for initial estimation of aerodynamic characteristics. The design is simulated in the system simulation tool Hopsan where a mission of the complete aircraft system can be simulated. Furthermore, it can be used to make an initial study of the control system in order to assess the feasibility of the concept, from a flight dynamics perspective.

1.1 Engine-Airframe Co-Design

It is likely, or at least desirable, that this development would include also the development of a dedicated engine. In this way the trade-off between engine cross-section regarding engine efficiency and airframe drag can be studied and balanced [2].

1.2 Basic Aerodynamic/Control Concept

As a concept close to the intended layout, the McDonnell Douglas X-36 [3] had been used as a start guess for the design. The main difference is the engine outlet which is projected to be a 2-axis thrust vector nozzle (TVN) compared with the stealth design engine outlet on the X-36. The scaled model of X-36 for future fighter concept will henceforth be termed as FX5 for all future references in this paper.

This project is intended to prove and assess the possibility of yaw control of a tailless configuration by the ailerons and TVN; with the help of simulations, the requirements regarding dynamic and deflection angles of the TVN should be stated. As complement for low thrust or engine out, flight conditions differential canard operation is suggested (see [4]) for side force generation. This is particularly efficient at high alphas. Furthermore, there is also the possibility to use differential ailerons/elevons or split ailerons.

1.3 Analysis of the X-36

With help of a 3-side drawing Fig. 2 and pictures, the basic X-36 geometry was modelled in both,

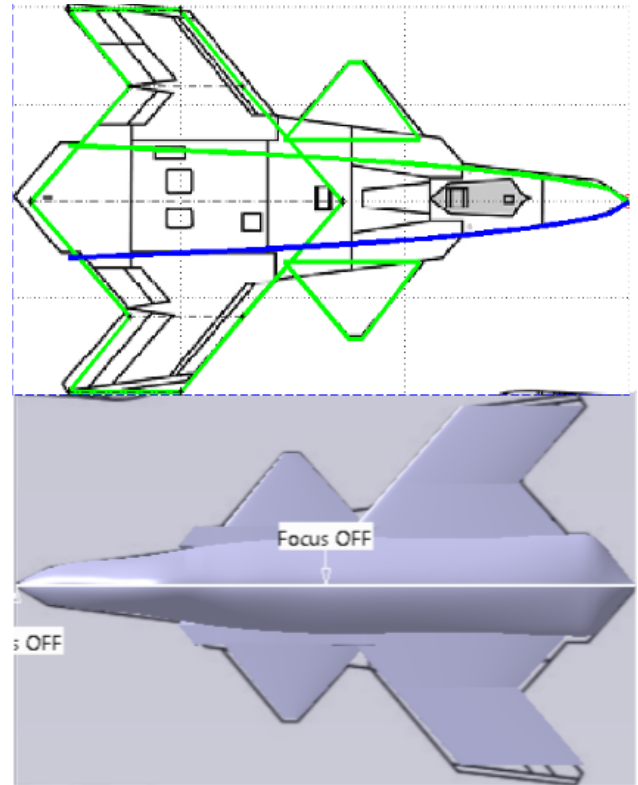


Fig. 2 : X-36 mapping in Tango(Top) and RAPID (Bottom).

sub-scale demonstrator (28% scale) and full size model.

2 Aerodynamic modelling

The geometry is modelled in Tornado [5], a vortex lattice method (VLM) implemented in Matlab. The method is a straightforward VLM with the standard assumptions: The wing is thin and at small angles of attack, the flow is incompressible and inviscous. Although these restrictions are quite extensive, the results may be corrected for compressibility effects for high subsonic Mach numbers ($M < 0.7$).

Viscous effects may be modeled using either a flat plate analogy, using a drag component build-up, or a 2D wing profile panel method coupled as a strip theory implementation. The 2D panel method uses a one-way coupled boundary layer model which does not require an iterative process. The wake may either be a rigid, fixed wake or a flexible, free-stream following wake. Tornado allows a user to define most types

of contemporary aircraft designs with multiple wings both cranked and twisted with multiple control surfaces. Each wing may have cranked taper of both camber and chord (Fig. 3).

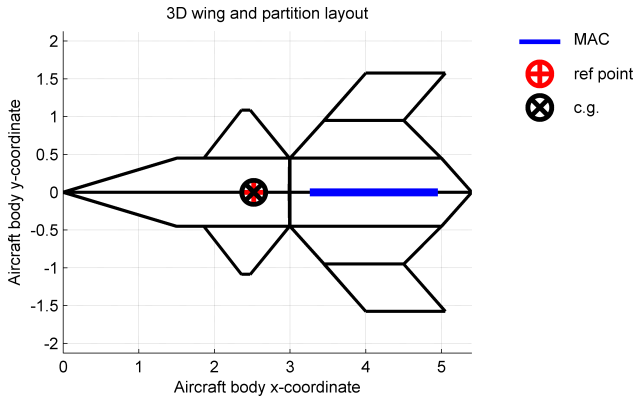


Fig. 3 : X-36 wing layout as rendered in Tornado.

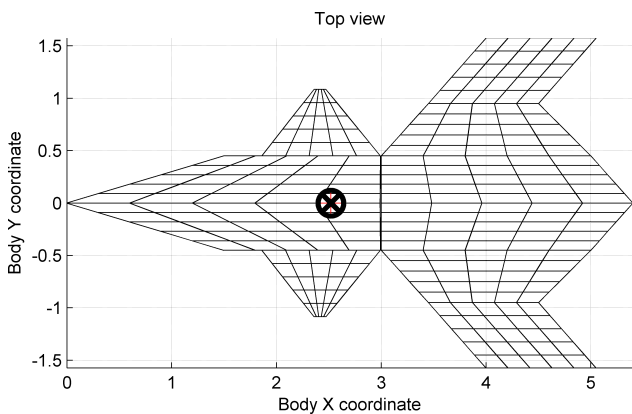


Fig. 4 : X-36 paneling with converged grid distribution.

When initializing the optimization loop (in this case canard angle to trim), the user should perform a grid convergence study to set the appropriate panel distribution in the aerodynamic computational mesh, or lattice. Tornado allows this to be done in an automated fashion. To ascertain good quality results, the grid convergence study should be performed at the end of the optimization loop to verify that any geometry changes made didn't affect the quality of the panel distribution. A typical convergence criterion is when the changes in lift, drag and pitching moment are lower than 1% between two iterations. The resulting grid distribution for the X-36 case can be seen in Fig. 4.

TORNADO CALCULATION RESULTS, Derivatives
 JID: a2
 Reference area: 4.8175 α [deg]: 4.466 P [rad/s]: 0
 Reference chord: 1.6911 β [deg]: 0 Q[rad/s]: 0
 Reference span: 3.15 Airspeed: 54.54 R[rad/s]: 0

CL derivatives :		CD derivatives :		CY derivatives :	
CL $_{\alpha}$	1.6349	CD $_{\alpha}$	0.0078611	CY $_{\alpha}$	-5.6801e-014
CL $_{\beta}$	4.5555e-009	CD $_{\beta}$	2.453e-009	CY $_{\beta}$	-3.1288e-014
CL $_P$	-4.1406e-008	CD $_P$	5.4618e-007	CY $_P$	-0.013542
CL $_Q$	4.9907	CD $_Q$	0.28516	CY $_Q$	2.3425e-012
CL $_R$	-8.6502e-011	CD $_R$	-7.1334e-012	CY $_R$	1.0318e-005

Roll derivatives :		Pitch derivatives :		Yaw derivatives :	
Cl $_{\alpha}$	2.6964e-013	Cm $_{\alpha}$	-0.00022971	Cn $_{\alpha}$	-1.7765e-014
Cl $_{\beta}$	1.5936e-013	Cm $_{\beta}$	-2.1697e-008	Cn $_{\beta}$	-2.4538e-015
Cl $_P$	-0.2167	Cm $_P$	-7.9846e-010	Cn $_P$	-0.011547
Cl $_Q$	-4.8008e-012	Cm $_Q$	-3.7853	Cn $_Q$	1.8756e-012
Cl $_R$	2.8636e-005	Cm $_R$	5.9508e-011	Cn $_R$	4.2417e-006

Fig. 5 : A typical Tornado output screen.

Fig. 5 shows a pitch trimmed case at 4.5 degrees angle of attack. The principal damping derivatives in roll and pitch are positive, but the lack of a vertical tail gives a diminutive positive yaw damping derivative. The static margin is close to zero, which is evident in the small pitching moment derivative with respect to angle of attack.

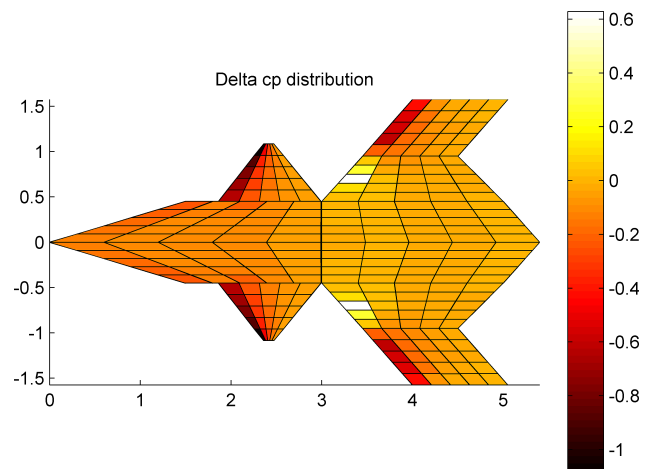


Fig. 6 : Pressure distribution of the Tornado X-36 model at 4.5 degrees angle of attack, pitch trimmed. Note the influence of the canard tip vortices on the main wing.

Tornado delivers the aerodynamic coefficients and control power derivatives needed for the systems and mission simulation. The aero data can either be delivered as a linearized point in the state space, with associated derivatives, or as a state database covering a larger area. Typically, only point data are needed to evaluate spe-

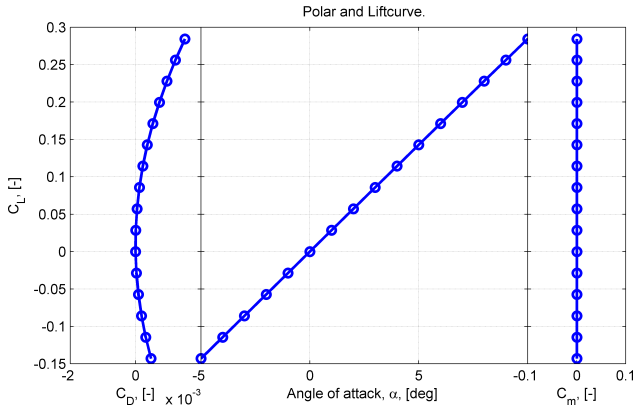


Fig. 7 : Drag polar for the X-36 model. Note that friction drag is not included.

cific mission segments such as: cruise, max maneuver, standard rate turn, etc. Fig. 5 show a typical Tornado output screen, in this instance for a low speed forward flight In pitch trim. The pressure distribution of the same case is shown in Fig. 6, where the influence of the tip vortices of the canards is clearly visible on the pressure distribution of the main wing. The drag polar for a- trimmed alpha sweep is shown in Fig. 7.

As shown in Fig. 8 with the center of gravity in the neutral point, no deflection was needed. With the CG forward of the NP, the pitching moment derivative with respect to angle of attack is negative and the limiting factor is the maximum allowable canard deflection. With the CG behind the NP, creating an unstable configuration, the needed deflections for trim is a lot smaller. However, since the Cm_{α} is negative, the limiting factor is the deflection rate of the canard surface. The use of a canard in the same plane as the main wing is therefore preferably operated in the unstable configuration as this gives a more linear control characteristic, and the slightly negative incidence of the canard compared to the main wing, will send the tip vortices on-top of the main-wing producing a greater CL max. The coefficients of the FX5 and X-36 are assumed to be similar as it is scaled-up from the X-36.

3 KBE for Fighter Geometric Design

Knowledge-based engineering has evolved during the years and it has been shown different

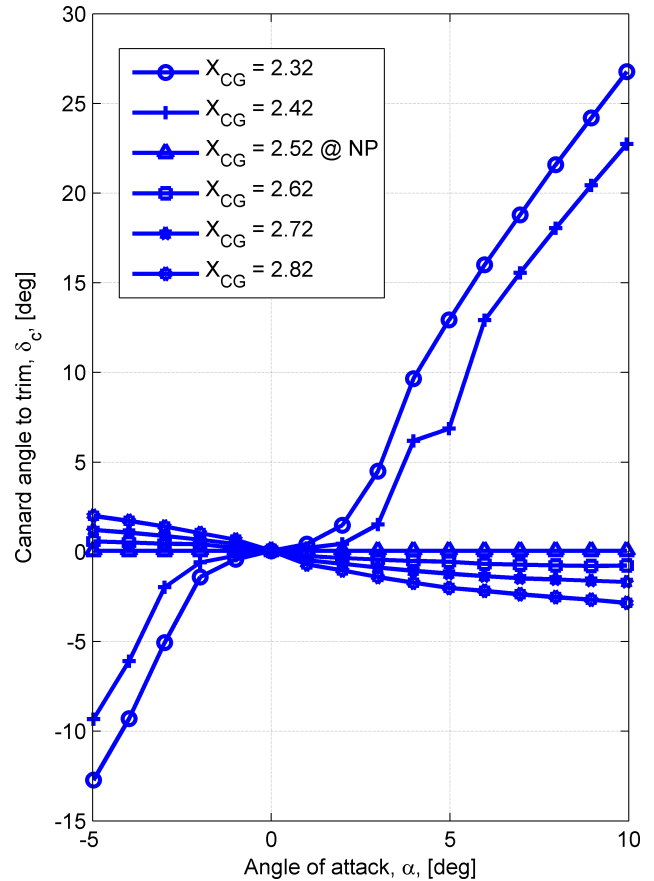


Fig. 8 : Canard deflection to trim for different CG positions on the X-36.

methods[6] [7][8] to implement and its applications in the aircraft industry. In addition to the method presented in [6], more sophisticated air intake and canopy design are added to RAPID for the FX5 fighter concept (Fig. 9).

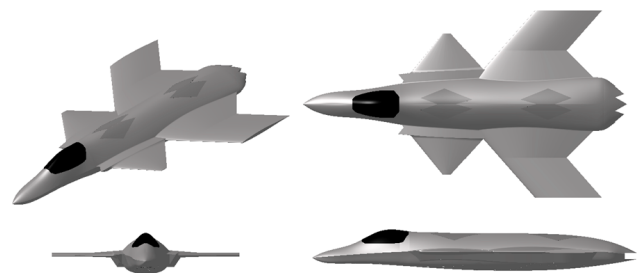


Fig. 9 : 3-views of the fighter aircraft concept FX5

3.1 Air intakes

The main purpose of intakes is to supply the engine with undisturbed airflow over the whole

flight envelope. There are different types of air intakes to study during the design process. In this case, the ramp inlet considered for conceptual design and eventually designed in RAPID. Capture area calculations implemented using the empirical equations [9] [10]. A S-duct is designed around the F110-132 engine and the fuselage tweaked around to obtain a stealth fighter for the future. Required number of sections needed can be chosen and the cross-section (similar to the fuselage cross-section [11]) can be modified after the instantiation, depending on the necessity.

3.2 Canopy Design

Two canopy designs can be designed in RAPID, Conventional and Blended canopy (Fig. 10). The canopy is designed by placing the pilot eye position and checked for minimum visibility criteria [12]. A mock-up of the pilot is used for the ergonomic study (Fig. 11) which further helps in the design of the cockpit.

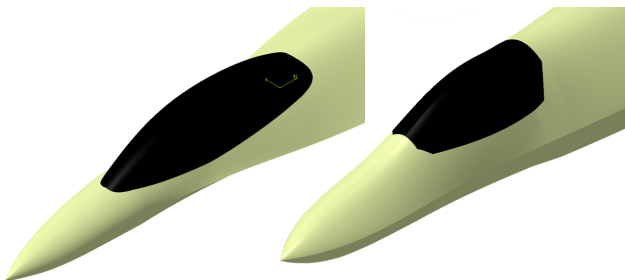


Fig. 10 : Left: Conventional canopy for a twin seat fighter. Right: Fuselage Blended canopy for a single seat fighter.

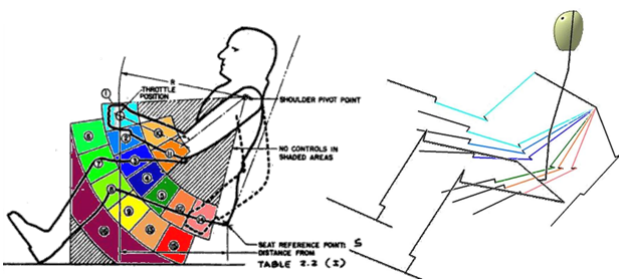


Fig. 11 : Left: Areas of good and poor accessibility in color code [12] and the arm positions color coded in RAPID[13]

4 Drag Prediction

An important aspect of the drag prediction is the wave drag, since this is critical to the aircraft's capability to achieve super cruise. From the RAPID software the area distribution (Fig. 12) for different Mach number can be calculated.

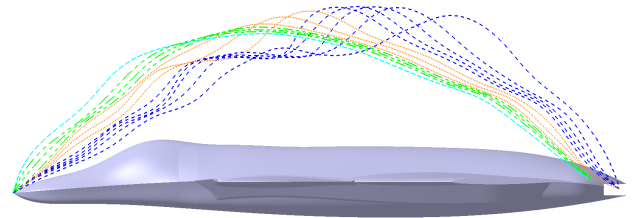


Fig. 12 : Effective Mach Cone area distribution for different Mach numbers ranging from 1 to 1.4; 1.6 to 2; 2.1 to 2.3 and 2.5.

There are two different methods to calculate the area distribution from the geometry available in RAPID, namely Plane average method and Mach cone Method. Mach Cone Method is elaborated in the session below, for more information on the Plane Average method refer [14]. Mach cone method is presented is similar to NACA Report [15] the following steps are followed to obtain the areas to calculate the wave drag.

- Cones are created with the defined Mach angle.
- The created cones are intersected with the aircraft geometry to get to the intersections.
- This intersected areas are then projected onto the plane perpendicular to the direction of flight.
- The areas are measured and normalized lengths of the areas are calculated. With this length a point is created in the Z-direction. Finally, all the points are joined to get the profile of the area distribution at each section as shown in Fig. 12.
- The areas obtained are used for the wave drag analysis.

4.1 Wave Drag Estimation

The wave drag is estimated using different empirical equations [9] [16] [17]. Fig. 13 and Fig. 14 shows the table of wave drag and its coefficients for different Mach numbers at sea level and at 12000 ft. The following equations are used to calculate the wave drag for full scale FX5.

CDwave for Sears-Haack bodies

$$CD_{wave} = \frac{4.5 * \pi}{S} * \left(\frac{A_{max}}{l} \right)^2 \quad (1)$$

$$A_{max} = \text{Maximum Cross - Section Area}$$

$$l = \text{Aircraft Length}$$

$$S = \text{Wing Reference Area}$$

CDwave for aircraft

$$CD_{wave} = \frac{4.5 * \pi}{S} * \left(\frac{A_{max}}{l} \right)^2$$

$$* (E_{WD} * 0.74 * 0.37 * \wedge_{LE})$$

$$* [1 - 0.3 * \sqrt{(M - M_{CD_{o,max}})}] \quad (2)$$

Equation (2) is only valid for

$$M_{\infty} \geq M_{CD_{o,max}} \quad (3)$$

$$M_{CD_{o,max}} = \frac{1}{\cos^2(\wedge_{LE})} \quad (4)$$

$$CD_{wave} = \frac{E_{WD}}{S} * [1 - (M - 1.2)^{0.57}]$$

$$* \left(1 - \frac{\pi * \wedge_{LE}(\text{degree})^{0.77}}{100} \right) * \left(\frac{D}{q} \right)_{\text{Sears-Haack}} \quad (5)$$

Equation (5) is only valid for

$$M \geq 1.2 \quad (6)$$

and finally

$$CD_{wave} = \frac{128 * V^2}{\pi' l^4 * S} \quad (7)$$

Mach	D/q_ Sears Haack	D/q_ wave	CD wave	Wave Drag (lbf)	Wave Drag (N)	Wave Drag (kgf)
1.2	1.04843	0.8457	0.0263	19360.35	87990.86	8978.66
1.3	1.04843	0.7579	0.0235	20360.91	92538.3	9442.68
1.4	1.04843	0.7153	0.0222	22287.34	101293.7	10336.09
1.6	1.04843	0.6521	0.0202	26537.94	120612.24	12307.37
1.8	1.04843	0.6018	0.0187	30993.86	140863.99	14373.88
2	1.04843	0.5583	0.0173	35499.47	161341.51	16463.42
2.1	1.04843	0.5383	0.0167	37738.72	171518.69	17501.91
2.2	1.04843	0.5193	0.0161	39954.39	181588.7	18529.46
2.3	1.04843	0.5011	0.0156	42136.46	191505.96	19541.42
2.5	1.04843	0.4666	0.0145	46361.9	210710.16	21501.04

Fig. 13 : Mach number versus Wave Drag Coefficient and Drag estimation at sea level

Mach	D/q_ Sears Haack	D/q_ wave	CD wave	Wave Drag (lbf)	Wave Drag (N)	Wave Drag (kgf)
1.2	1.04843	0.8457	0.0263	3598.23	16011.3	1633.81
1.3	1.04843	0.7579	0.0235	3784.19	16838.8	1718.24
1.4	1.04843	0.7153	0.0222	4142.22	18432	1880.81
1.6	1.04843	0.6521	0.0202	4932.22	21947.3	2239.52
1.8	1.04843	0.6018	0.0187	5760.38	25632.4	2615.55
2	1.04843	0.5583	0.0173	6597.77	29358.6	2995.78
2.1	1.04843	0.5383	0.0167	7013.95	31210.5	3184.74
2.2	1.04843	0.5193	0.0161	7425.74	33042.9	3371.72
2.3	1.04843	0.5011	0.0156	7831.29	34847.5	3555.87
2.5	1.04843	0.4666	0.0145	8616.61	38342	3912.45

Fig. 14 : Mach number versus Wave Drag Coefficient and Drag estimation at 12000 ft

5 Mission Simulation

For evaluating the performance of the aircraft in a realistic scenario a system simulation [18] model was built that could be used in a mission simulation. The flight dynamics model is here based on a 6 degree of freedom rigid body model that is connected to an aerodynamic model. The aerodynamic model (Fig. 15) can have different number of wings, with an arbitrary number of control surfaces, and a body with its characteristics. It is here based on a static version of the model presented in [19], although the unsteady effects can of course also be included.

The control surfaces are modelled both with a linear increase of lift force with deflection and the corresponding increase in induced drag. There is also a cross coupling effect of drag for control surfaces on the same wing e.g. ailerons and flaps. In this way also the effect of trim drag on performance is automatically included, and the effect

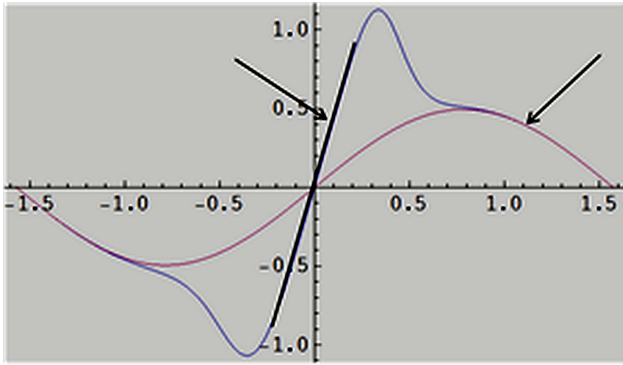


Fig. 15 : Non-linear aerodynamic model.

of reduced weight as fuel is consumed. The system (Fig. 16) also includes a simple control system and a mission model, and the Dryden atmospheric wind gust model is implemented, There is also a simple gas turbine models that produce thrust and fuel consumption as a function of density, temperature and speed. The engine model is based on the GE F110-132 engine. A future engine would have even more thrust but this is used as a conservative estimate. The hydraulic actuation (Fig. 17) system is also modelled in some detail to make sure that subsystem performance is adequate. In this way effects of failure modes can be simulated. The system is implemented in the Hopsan simulation package developed at Linköping University.

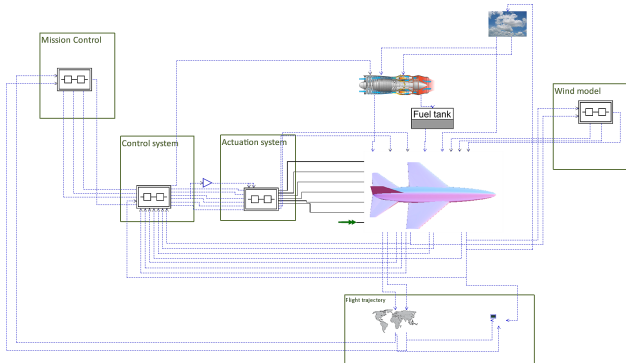


Fig. 16 : Hopsan system simulation model.

There is a hierarchical model of the hydraulic actuation system so that basic performance and some failure modes can be studied.

A basic flight control system is implemented so that controllability can be studied already at the conceptual design stage. This is particularly important when unconventional concepts

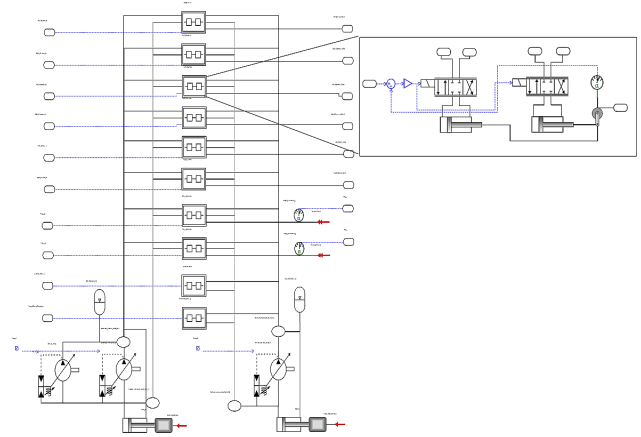


Fig. 17 : Hydraulic actuation system.

are studied. Here a simulation of a S-maneuver (Fig. 18) was performed to check transient performance and controllability. The aircraft then transit to post stall flight going from a speed of 225 m/s down to 55 m/s (Fig. 19) using the thrust vector control for STOVL performance. Since this configuration is tailless, alternative yaw control methods have to be used.

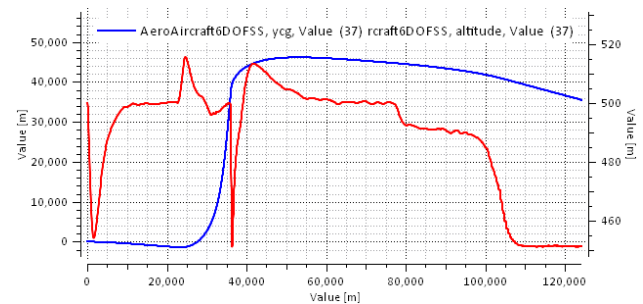


Fig. 18 : Flight trajectory of S-maneuver and subsequent transition to post-stall flight. (Drift is due to side wind)

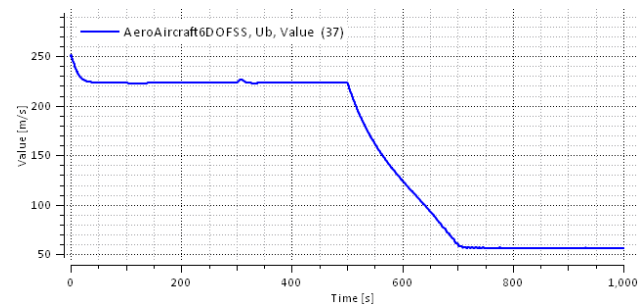


Fig. 19 : Speed during the S-maneuver and post stall flight.

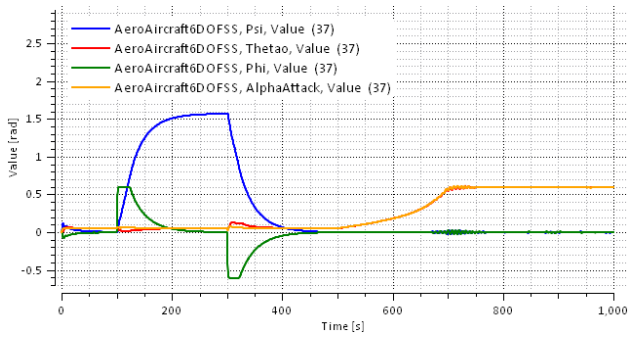


Fig. 20 : Attitude angles during S-maneuver and subsequent transition to post-stall flight using trust vectoring.

In this case there is thrust vectoring (Fig. 20) as a primary means of yaw control. In addition canard can be used in a differential way and thereby create a side force as studied in [4]. This is needed at low trust settings and in engine out situations. As a fall-back also split ailerons can also be used to create yaw stability at the expense of drag.

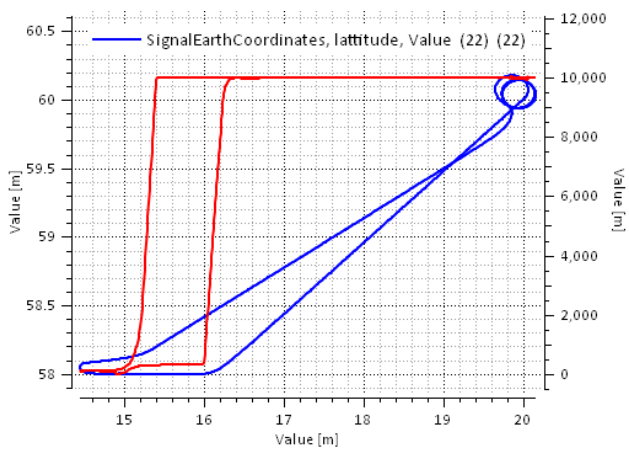


Fig. 21 : Simulated combat mission with high speed outgoing and subsonic cruise on the return.

In addition to simulations in order to study flight dynamics and control a simulation of a design mission (Fig. 21) and speed profile (Fig. 22) can be performed using the same model. The design mission is a clean high altitude intercept mission with a super-cruise to the target area and a subsonic return flight. Two main evaluation criteria are the mission time and the consumed fuel.

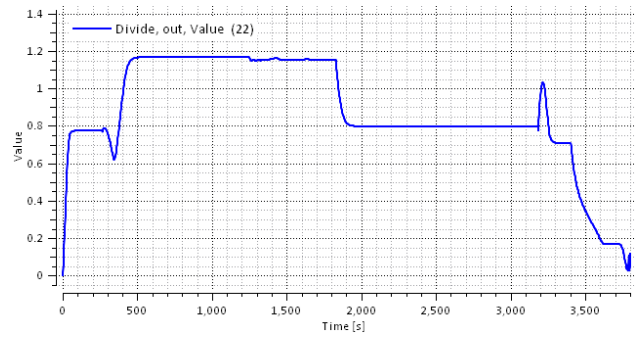


Fig. 22 : Speed profile (Mach number) during the mission. Total time of mission 3900 sec.

6 Conclusion

A knowledge-based future fighter concept is presented in this paper. Firstly, the scaled model of X-36 is designed in Tornado and Tango. This model is then scaled up by a factor of 2.5 to obtain FX5, the fuselage is modified and weapon-bay size is reduced for future weapon integrations. It has been observed that for a full scale model of X-36 there could be a twin engine, for the purpose of FX5 only one engine is installed with thrust vectoring. This will enable for a light weight structure for a single seater or pilot-less aircraft, reduced radar cross-section signature and increased super cruise capability. The pilot-less aircraft is assumed to be fitted with a state-of-the-art Laser Weapon System for future weapon integrations. The future fighter concept has been proven in the mission simulation of FX5.

References

- [1] Jouannet C and Krus P. Unsteady aerodynamic modelling: a simple state-space approach, *AIAA Aerospace sciences meeting and exhibit*, Reno, USA, 2005.
- [2] Abdalla A, Gazetta H, Grönstedt T and Krus P. The Effect of Engine Dimensions on Supersonic Aircraft Performance, *4th CEAS Air & Space Conference*, Linköping, Sweden, 2013.
- [3] <http://www.nasa.gov/centers/armstrong/multimedia/imagegallery/X-36/>, last accessed 07th July 2014.
- [4] Re R J and Capone F J. *An Investigation of a Close-coupled Canard As a Direct Side-force*

- Generator On a Fighter Model At Mach Numbers from 0.40 to 0.90.*, Technical Note, L-11613, National Aeronautics and Space Administration, Washington, USA, 1977.
- [5] Melin T. *TORNADO - A Vortex-Lattice Matlab implementation for linear aerodynamic wing applications*, Master Thesis, Department of Aeronautics, Royal Institute of Technology (KTH), Stockholm, Sweden, 2000.
- [6] Munjulury R C. *Knowledge Based Integrated Multidisciplinary Aircraft Conceptual Design*, Licentiate Thesis No. 1661, Institute of Technology, Linköping University, Sweden, 2014
- [7] La Rocca G. and Van Tooren M J L. Enabling distributed multi-disciplinary design of complex products: a knowledge based engineering approach. *Journal of Design Research*, Vol. 5, No. 3, pp 333-352, 2007.
- [8] Amadori K, Tarkian M, Ölvander J and Krus P. Flexible and Robust CAD Models for Design Automation. *Advanced Engineering Informatics*, Vol. 26, No. 2, pp 180-195, 2012.
- [9] Raymer D. *Aircraft design - A Conceptual Approach*, AIAA education series, Washington DC, USA, 2012, ISBN: 978-1-60086-911-2.
- [10] Seddon J and Goldsmith E L. *Intake aerodynamics*, 2nd ed, Blackwell Science, Oxford, 1999, ISBN: 978-0-632-04963-9.
- [11] Staack I, et al. Parametric Aircraft Conceptual Design space, *Proceedings of the 28th Congress of the International Council of the Aeronautical Science*, Brisbane, Australia, 2012
- [12] Roskam J. *Airplane design, Part III: Layout of Cockpit, Fuselage, Wing and Empennage: Cutaways and Inboard Profiles*, Roskam Aviation and Engineering Corporation, Kansas, USA, 1989.
- [13] Tassel W. *Development of a Complete Parametric CAD Model of a Cockpit Layout for Civil Airplane under CATIA CAD Software*, Masters thesis, Linköping University, Sweden, 2010.
- [14] Staack I, Munjulury R C, et al. Conceptual Design Model Management Demonstrated on a 4th Generation Fighter, *Proc 29th Congress of the International Council of the Aeronautical Science*, St. Petersburg, Russia, 2014.
- [15] Robert T. Jones, *Theory of Wing-Body Drags at Super Sonic Speeds*. NACA Rept. 1284, 1953.
- [16] Brandt S A, Stiles R J, Bertin J J and Whitford R. *Introduction to Aeronautics - A Design Perspective*, 2nd ed, AIAA education series, Washington DC, USA, 2004, ISBN: 978-1-56347-701-0.
- [17] Rallabhandi S K and Mavris D N. An Unstructured Wave Drag code for the Preliminary Design of Future Supersonic Aircraft, *33rd AIAA Fluid Dynamics Conference and Exhibit*, Orlando, FL, USA, 2003.
- [18] Krus P, Braun R, Nordin P and Eriksson B. Aircraft System Simulation for Preliminary Design, *28th Congress of the International Council of the Aeronautical Sciences*, Brisbane, Australia, 2012.
- [19] Barger R L and Adams M S. *Fuselage Design for a Specified Mach-Sliced Area Distribution*, NASA Technical Paper 2975, Langley Research Center, Hampton, Virginia.

7 Contact Author Email Address

petter.krus@liu.se

Copyright Statement

The authors confirm that they, and/or their company or organization, hold copyright on all of the original material included in this paper. The authors also confirm that they have obtained permission, from the copyright holder of any third party material included in this paper, to publish it as part of their paper. The authors confirm that they give permission, or have obtained permission from the copyright holder of this paper, for the publication and distribution of this paper as part of the ICAS 2014 proceedings or as individual off-prints from the proceedings.